SEVENTH FRAMEWORK PROGRAMME
THEME 3
ICT - INFORMATION AND COMMUNICATION TECHNOLOGIES

Project acronym:	AEOLUS
Project full title:	Distributed Control of Large-Scale Offshore Wind Farms
Project reference:	**224548**
Start date:	1 May 2008
Duration:	41 months

Deliverable no.: 4.4

Title: Adaptive reconfiguration for robustness and fault-tolerance

Contractual date of delivery:	30. September 2011
Actual date of delivery:	30. September 2011
Lead beneficiary of this deliverable:	ULUND
Author(s):	M. Kristalny, D. Madjidian, A. Rantzer
Participant(s):	M. Kristalny, D. Madjidian, A. Rantzer
Work packages contributing to the deliverable:	WP4
Nature:	R
Version:	1.0
Total number of pages:	22
Dissemination level:	PU

Summary:
This deliverable has significantly benefited from the recruitment of Maxim Kristalny as a postdoc from Technion (Israel). The recruitment created an unexpected opportunity to exploit recent research developments on the systematic use of preview information for feedforward control. It is a well known fact in control engineering that significant benefits often can be achieved by complementing feedback control with preview information (feedforward) about known disturbances. In wind farms, it is very natural to use wind speed measurements at upwind turbines as a source of preview information for feedforward control of downwind turbines. However, this information has traditionally not be exploited. There are several reasons for this, one of them being uncertain time-delays due to variations in speed and direction of the wind. Traditional methods to handle such variations lead to very complicated models and control laws.
A newgeneration of feedforward control techniques have been developed over the past few years, with Kristanly's PhD thesis being an important milestone. By exploiting these methods for wind farm control in this deliverable, we hope to lay the proper foundation for future wind farm control structures, with improved performance, robustness and adaptability as consequence.

AEOLUS Deliverable 4.4

Adaptive reconfiguration for robustness and fault-tolerance

Maxim Kristalny
Daria Madjidian
Anders Rantzer

Automatic Control LTH
Lund University
September 2011

Preface

This deliverable has significantly benefited from the recruitment of Maxim Kristalny as a postdoc from Technion (Israel). The recruitment created an unexpected opportunity to exploit recent research developments on the systematic use of preview information for feedforward control.

It is a well known fact in control engineering that significant benefits often can be achieved by complementing feedback control with preview information (feedforward) about known disturbances. In wind farms, it is very natural to use wind speed measurements at upwind turbines as a source of preview information for downwind turbines. The preview information gives improved adaptation to wind-variations. It also improves the fault-tolerance, since a fault in one row of turbines is detected through wind speed measurements in the next row and compensated further downwind using the preview information.

In spite of the great potential, preview information has traditionally not be exploited. There are several reasons for this, one of them being uncertain time-delays due to variations in speed and direction of the wind. Traditional methods to handle such variations lead to very complicated models and control laws. However, a new generation of feedforward control techniques have been developed over the past few years, with Kristanly's PhD thesis being an important milestone. By exploiting these methods for wind farm control in this deliverable, we hope to lay the proper foundation for future wind farm control structures, leading to improved adaptability, robustness and fault-tolerance.

Anders Rantzer
leader of WP4

1 INTRODUCTION

In the past decade wind power capacity has continued to grow at an annual rate of 30% [1]. Economy of scale makes it attractive to position turbines close to each other, forming large-scale wind farms [2]. Such placement may cause various difficulties due to wake effects [3, 4]. However, it also offers a possibility to communicate with and to account for the neighbouring turbines. This can be exploited for reducing the loads experienced by the turbines.

Most of the research devoted to control of wind turbines for load mitigation focuses on a single turbine, see [5, 6, 2] and the references therein. Yet, as mentioned above, it might be advantageous to consider problem formulations that take the entire farm into account. The potential benefits of such formulations are:

- The ability to share wind measurements among adjacent turbines in the farm. In this setting, downwind turbines can use upwind turbines as sensors that provide preview of the upcoming wind speed.

- The possibility for turbines to cooperate in terms of power production. This may introduce more freedom in adjusting individual turbine power and can be exploited for load reduction.

In the current report we examine the possibility of exploiting these benefits using a distributed feedforward control scheme. An illustrative setup of collective-pitch power controlled turbines arranged in a row is considered, as in [7]. The potential of the proposed control strategy is assessed and several theoretical challenges are outlined.

In the first part of the report we focus on the idea of exploiting previewed wind speed measurements for reducing the loads experienced by an individual turbine. In wind farms such a preview can be obtained from upwind turbines. However, one may also think of other sources, such as LIDAR systems [8]. The idea of using preview in control of wind turbines was discussed in [9]. Yet, so far, only a few results are available on this topic, [10, 11], based on discrete time H^∞ and model predictive control. We adopt a different approach and show that the problem can be conveniently formulated as a continuous time H^2 model matching optimization. We solve it using recent results from [12] and present simulations demonstrating the optimal controller behavior. The simulations indicate that thrust force fluctuations and the associated tower oscillations can be significantly reduced by adjusting turbine power in response to upcoming wind conditions. The influence of preview length on the performance is analyzed.

In the second part of the report we explore the benefits of cooperation between turbines in the farm. As wind farms become more common, they are expected to contribute to the stability of the electrical grid, meaning that they should be able to receive and maintain power set points. This impedes load mitigation, since it restricts turbines in adjusting their power production. Cooperation between turbines adds flexibility by allowing power to be redistributed between the turbines. This can be advantageous since wind conditions across

the farm are not uniform. Thus, once wind conditions in one region of the farm suggest changes in power production, turbines in other regions may compensate for these changes. Coordination of turbine powers within the farm for load mitigation has been studied in [13] and [7]. In [13] the aero-dynamic coupling between turbines is neglected, and a centralized receding horizon control scheme is proposed. In [7] restrictions on communication between turbines are imposed and a distributed control synthesis method is used to obtain distributed state feedback controllers. As in [7], we consider a decentralized setting and allow communication only between adjacent turbines. However, we assume that only wind speed measurements (as opposed to the entire state vector in [7]) are communicated. We show that under a reasonable assumption, the problem is essentially a feedforward problem and can be formulated as a decentralized H^2 model matching optimization. A number of fundamental challenges associated with it are outlined and possible remedies are discussed. The ideas from [14] are exploited to find an approximate frequency domain solution. This is used to obtain preliminary simulation results, which reveal the nature of cooperation between turbines under the proposed control strategy.

This report is organized as follows. The models of an individual turbine and a complete farm are described in Section 2. Section 3 focuses on feedforward control of an individual turbine based on previewed wind speed measurements. Section 4 is devoted to the distributed feedforward control of an entire farm. Finally, some concluding remarks are available in Section 5.

Notation Given a transfer matrix $G(s)$, its conjugate is denoted by $G^{\sim}(s) := [G(-s)]'$. If $G \in L^2$, $\{G\}_-$ and $\{G\}_+$ refers to the projection of G onto H^2 and $H^2_\perp$ respectively. The Kronecker, Khatri-Rao and Hadamard (entry-wise) products of two matrices are denoted by $A \otimes B$, $A \odot B$ and $A \circ B$, respectively. The vector operator $\mathrm{vec}(A)$ denotes a vector formed by stacking all columns of A. For a diagonal matrix $D = \mathrm{diag}(d_1, \ldots, d_n)$, the notation $\mathrm{dvec}(D) := \begin{bmatrix} d_1 & \cdots & d_n \end{bmatrix}'$ is used.

2 MODELING

2.1 Turbine model

In this work we use a simplified third order model of an NREL 5MW turbine, equipped with a standard internal controller, see [15] and [13]. The internal controller manipulates the generator torque and the blade pitch angle in order to meet a prescribed power demand. It has three main modes of operation, usually called "operating regions". The first mode is active when the wind speed is lower then some minimum level required for power production. In this situation the controller freezes the rotor motion and no power is produced. The second mode is active when the demand of power is higher than the power available in the wind. In this mode the controller captures maximum power by fixing the pitch angle and adjusting the generator torque to attain the optimal

rotor speed. The controller operates in the third mode if the power demand is lower than the power that can be captured by the turbine. In this mode the controller keeps the rotor speed close to its rated value by modifying the pitch angle. The generator torque is then manipulated to maintain the level of the produced power. We will assume that the power demand does not exceed the maximal power that can be extracted from the wind. Hence, it will be assumed hereafter that internal controllers are in the third mode.

Denote the nominal mean wind speed and power demand by V_{nom} and p_{nom}. A linearized model of a turbine near its operating point can be described by a continuous time LTI system depicted in Figure 1. It can be partitioned as $P = \begin{bmatrix} P_V & P_u \end{bmatrix}$ with respect to the input signals. The inputs V and p_{ref} denote deviations in the wind speed and the power demand from their nominal values. The second input will also be denoted as $u := p_{\text{ref}}$. Note that in the considered setting u is the only available control signal.Neglecting the generator dynamics, we will assume the actual deviation in power production equals p_{ref}. The outputs F, T, w, and β are the deviations in the thrust force, rotor shaft torque, rotor speed, and pitch angle, respectively. The vector containing all outputs of the system will be denoted by $z := \begin{bmatrix} F & T & w & \beta \end{bmatrix}'$.

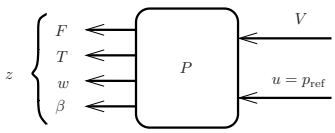

Figure 1: Separate turbine

We will consider tower oscillations as an external dynamical mode induced by the thrust force. It will be approximated by a second order system with natural frequency $\omega_{\text{twr}} = 2$ rad/sec and damping coefficient $\zeta_{\text{twr}} = 0.08$. Similarly, rotor shaft oscillations induced by the torque will be approximated by a second order system with $\omega_{\text{sft}} = 14$ rad/sec, and $\zeta_{\text{sft}} = 0.05$. The values above were calculated based on [15].

Remark 1 *Considering a turbine equipped with a standard internal controller is restrictive, as it rules out direct access to the pitch and the generator torque. On the other hand, this setup has two benefits. First, it simplifies the problem, enabling us to concentrate on the central issues addressed in this report. Second, it facilitates experiments in existing wind farms by releasing the need in hardware replacement. We would also like to add that the ideas, the problem formulations and the open challenges raised below can naturally be extended to more general situations with no internal controller and/or individual pitch capabilities.*

2.2 Wind farm model

We consider a row of N equidistant turbines and assume wind direction to be parallel to the row, see Figure 2.

Coupling between turbines due to wake effects plays an important role in quasi-static analysis of wind farms [3]. However, once the dynamic behavior of turbines is considered in the vicinity of an operating point, these effects become less relevant. Practical studies suggest that variations in wind speed caused by

Figure 2: One-dimensional wind farm topology

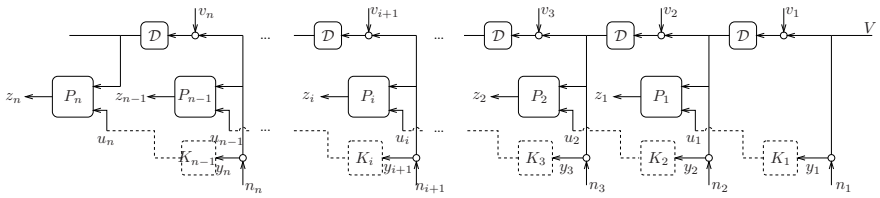

Figure 3: Block diagram of a wind farm (solid) and distributed feedforward control scheme (dashed)

turbines pitching are small compared to the natural variation in the wind [16]. Motivated by this we will neglect the influence of pitch activity on the wind flow and model the propagation of wind deviations between adjacent turbines by a delay and additive noise.

Following the discussion above, a wind farm can be described by the block diagram depicted in Figure 3 with solid lines. Systems P_i in this diagram stand for turbine models, linearized around their operating points. Note that operating points of different turbines in a farm are different due to wake effects [17] and, as a result, the models P_i do not coincide. As in the previous subsection, turbine models will be partitioned with respect to their inputs $P_i = \left[\begin{smallmatrix} P_{i,V} & P_{i,u} \end{smallmatrix}\right]$. Signals u_i represent the control signals and constitute variations in turbines power production. The output of the turbine i is denoted by $z_i := \left[\begin{smallmatrix} F_i & T_i & w_i & \beta_i \end{smallmatrix}\right]'$, where the notations are consistent with those in the previous subsection. The deviation of the incoming ambient wind speed from its nominal value is denoted by V. The time delays associated with wind propagation are represented by $\mathcal{D} = \mathrm{e}^{-sh}$, where the delay length h represents the amount of time required for the wind to travel from a turbine to its closest downwind neighbor. The additive wind noises are denoted by v_i. Signals y_i represent wind speed measurements and n_i stand for the corresponding measurement noises.

The stacked vectors of measured signals, turbine outputs, and controls will be denoted by

$$\bar{y} := \begin{bmatrix} y_1 \\ \vdots \\ y_N \end{bmatrix}, \quad \bar{z} := \begin{bmatrix} z_1 \\ \vdots \\ z_N \end{bmatrix}, \quad \bar{u} := \begin{bmatrix} u_1 \\ \vdots \\ u_N \end{bmatrix}. \tag{1}$$

The vector of all exogenous signals will be denoted by

$$\bar{w} := \left[\begin{smallmatrix} V & v_1 & \cdots & v_N & n_1 & \cdots & n_N \end{smallmatrix}\right]'.$$

Let us define the systems

$$G_m := \left[\begin{array}{c:ccc:c:ccc} 1 & 0 & \cdots & 0 & 0 & 1 & 0 & \cdots & 0 \\ 1 & 1 & \ddots & \vdots & \vdots & 0 & 1 & \cdots & 0 \\ \vdots & \vdots & \ddots & 0 & 0 & \vdots & \vdots & \ddots & \vdots \\ 1 & 1 & \cdots & 1 & 0 & 0 & 0 & \cdots & 1 \end{array}\right]$$

$$G_c := \left[\begin{array}{ccc} P_{1,u} & \cdots & 0 \\ \vdots & \ddots & 0 \\ 0 & \cdots & P_{N,u} \end{array}\right]$$

$$G_w := \left[\begin{array}{c:ccc:c:ccc} P_{1,V} & P_{1,V} & 0 & \cdots & 0 & 0 & 0 & \cdots & 0 \\ P_{2,V} & P_{2,V} & P_{2,V} & \cdots & 0 & 0 & 0 & \cdots & 0 \\ \vdots & \vdots & \vdots & \ddots & 0 & \vdots & \vdots & \ddots & \vdots \\ P_{N,V} & P_{N,V} & P_{N,V} & \cdots & P_{N,V} & 0 & 0 & \cdots & 0 \end{array}\right]$$

where G_m has the dimension of $N \times 2N + 1$. Also define the multichannel diagonal delay element

$$\Lambda := \mathrm{diag}\{\mathcal{D}, \mathcal{D}^2, \ldots, \mathcal{D}^N\}.$$

The relations between the signals in the block diagram in Figure 3 are then given by the following expressions

$$\bar{y} = \mathcal{D}^{-1}\Lambda\bar{G}_m\bar{w}, \quad \bar{z} = G_c\bar{u} + \Lambda G_w\bar{w},$$

which will be used later on in Section 4.

3 FEEDFORWARD CONTROL OF AN INDIVIDUAL TURBINE

In this section we focus on the individual turbine behavior and study to what extent feedforward action based on wind measurements can be helpful for load mitigation. The main questions addressed in this section can be formulated as follows:

- Is it possible to reduce turbine loads by short term power adjustments with respect to the measured wind speed?
- To what extent is preview of the wind speed beneficial?

3.1 Problem formulation

The problem naturally falls into the open-loop measured disturbance attenuation scheme, depicted in Figure 4. The plant $\left[\begin{smallmatrix} P_V & P_u \end{smallmatrix}\right]$ represents the linearized turbine model, described in § 2.1. The wind speed deviation V acts as a disturbance measured with the noise n. The delay h in the first plant input corresponds to the length of preview available to the controller K. The aim of the

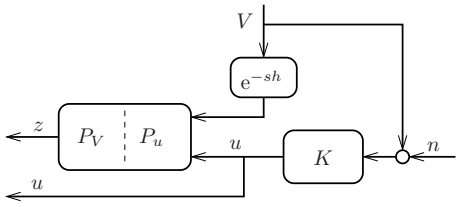

Figure 4: Open-loop measured disturbance attenuation scheme

controller is to keep the components of z small. Pitch activity should be kept low to reduce wear in the pitch mechanism. Deviations of rotor speed from its rated value should not be large due to mechanical design constraints. Finally, fluctuations in thrust force and shaft torque should be alleviated, since they introduce oscillations, which cause damage to the tower and rotor shaft [3]. To prevent large fluctuations in the produced power, the control signal u should also be penalized.

The relation between the input and output signals in Figure 4 is given by:

$$\begin{bmatrix} z/V & z/n \\ u/V & u/n \end{bmatrix} = \begin{bmatrix} e^{-sh}P_V & 0 \\ 0 & 0 \end{bmatrix} + \begin{bmatrix} P_u \\ 1 \end{bmatrix} K \begin{bmatrix} 1 & 1 \end{bmatrix}.$$

Define the cost transfer function for the optimization as

$$H := \begin{bmatrix} W_z & 0 \\ 0 & W_u \end{bmatrix} \begin{bmatrix} z/V & z/n \\ u/V & u/n \end{bmatrix} \begin{bmatrix} W_V & 0 \\ 0 & W_n \end{bmatrix},$$

where W_u, W_V and W_n are the weights for u, V and n, respectively, and $W_z = \text{diag}\{W_F, W_T, W_w, W_\beta\}$ contains weights for all the components of z. For simplicity, we let the input weights be static $W_V = k_V$, $W_n = k_n$. The weight of the thrust force is chosen as

$$W_F = k_F \frac{s + \omega_{\text{twr}}}{s^2 + \omega_{\text{twr}}^2}.$$

Note that it contains unstable poles on the imaginary axis, which correspond to the natural frequency of the tower. Together with input-output stability requirement on H, this imposes a constraint not to awake tower oscillations. Similarly, to account for shaft oscillations, we let

$$W_T = k_T \frac{s + \omega_{\text{shf}}}{s^2 + \omega_{\text{sft}}^2}.$$

The weights for the pitch angle and rotor speed are chosen to be static $W_\beta = k_\beta$, $W_w = k_w$. Finally, we choose

$$W_u = k_p \frac{(0.1s + 1)}{s} \cdot \frac{(s + \omega_{\text{twr}})^2}{s^2 + 0.02\ \omega_{\text{twr}} + \omega_{\text{twr}}^2}.$$

The integrator ensures zero steady-state power deviation in response to constant inputs. In other words, we do not allow the feedforward controller to shift the power set point even for permanent changes in wind conditions. The resonant peak of W_u prevents the controller from damping tower oscillations by means of oscillations in power production.

Defining the transfer matrices

$$\left[\begin{array}{c:cc} G_1 & G_3 \\ \hdashline G_2 & 0 \end{array}\right] := \left[\begin{array}{ccc:c} \mathrm{e}^{-sh}W_z P_V W_V & 0 & W_z P_u \\ 0 & 0 & W_u \\ \hdashline W_V & W_n & 0 \end{array}\right] \tag{2}$$

and choosing $||H||_2$ as the performance criterion, the problem can now be formulated as model matching optimization.

OP$_1$: Given G_1, G_2 and G_3 as defined in (2) find $K \in H^\infty$, which guarantees

$$H = G_1 - G_3 K G_2 \in H^2 \cap H^\infty \tag{3}$$

and minimizes $||H||_2$.

The formulation above can be considered as a unified setting for estimation and control problems with information preview and asymptotic behavior constraints, [12]. The stability requirement $H \in H^\infty$ accounts for the asymptotic performance. In our work, it reflects the requirements not to shift power set point and to cancel tower and shaft oscillatory modes. The minimization of $||H||_2$ accounts for the transient performance. Availability of preview is captured by the delay element in the definition of G_1 in (2).

3.2 Problem solution

Although availability of preview is a benefit that can potentially improve the performance, mathematically, it complicates the problem by rendering it infinite-dimensional. One of the ways to address this difficulty is by discretizing the time axes and treating the delay element on equal footing with the rest of problem dynamics, [7]. This approach, however, leads to a substantial increase of computational burden and is subject to numerical difficulties.

Efficient methods for the solution of a one-side version of **OP**$_1$, in which either G_2 or G_3 equal identity, are well studied, [18, 19]. Yet, their extension to the general two-sided setting is by no means trivial. Recently, a solution of a two-side problem was obtained in [12].

To present this result, consider the composite system $G = \left[\begin{smallmatrix} e^{sh}G_1 & G_3 \\ G_2 & 0 \end{smallmatrix}\right]$. Note that this system is finite-dimensional and, thus, can be given by its minimal state-space realization

$$G = \left[\begin{array}{c|cc} A & B_1 & B_3 \\ \hline C_1 & 0 & D_3 \\ C_2 & D_2 & 0 \end{array}\right] = \left[\begin{array}{ccc|cc} A_3 & A_{12} & A_{13} & B_{11} & B_{13} \\ 0 & A_{1\mathrm{i}} & A_{23} & B_{21} & 0 \\ 0 & 0 & A_2 & B_{31} & 0 \\ \hline C_{11} & C_{12} & C_{13} & 0 & D_3 \\ 0 & 0 & C_{23} & D_2 & 0 \end{array}\right],$$

where (A_3, B_{13}) and (A_2, C_{23}) are controllable and observable, respectively. Without loss of the generality, we may assume that the realization above has an additional structure:

$$\left[\begin{array}{c:c:c} A_3 & A_{12} & A_{13} \end{array}\right] = \left[\begin{array}{cc:c:cc} A_{3\mathrm{u}} & 0 & 0 & 0 & \times \\ 0 & A_{3\mathrm{s}} & \times & \times & 0 \end{array}\right]$$

$$\left[\begin{array}{c} A_{23} \\ \hdashline A_2 \end{array}\right] = \left[\begin{array}{cc} \times & 0 \\ \hdashline A_{2\mathrm{s}} & 0 \\ 0 & A_{2\mathrm{u}} \end{array}\right],$$

where $A_{2\mathrm{s}}$ and $A_{3\mathrm{s}}$ are Hurwitz, $A_{2\mathrm{u}}$ and $A_{3\mathrm{u}}$ are anti-stable, and "$\times$" stand for irrelevant blocks. In addition, we assume that

$\boldsymbol{\mathcal{A}_1}$: A has no eigenvalues in the open right-hand plane,

$\boldsymbol{\mathcal{A}_2}$: $D_2 D_2' = I$ and $D_3' D_3 = I$,

$\boldsymbol{\mathcal{A}_3}$: $G_2(s)$ and $G_3(s)$ have no jω-axis zeros.

Assumption $\boldsymbol{\mathcal{A}_1}$ is practically not restrictive, because unstable poles present in $\mathbf{OP}_1$ originate from unstable weights with imaginary axis instabilities. $\boldsymbol{\mathcal{A}_{2,3}}$ are standard assumptions in the H^2 optimal control guaranteeing well posedness.

Define matrices E_2 and E_3 through the equalities $A_2 E_2 = E_2 A_{2\mathrm{u}}$ and $E_3' A_3 = A_{3\mathrm{u}} E_3'$, i.e., $E_2 = \left[\begin{smallmatrix} 0 \\ I \end{smallmatrix}\right]$ and $E_3 = \left[\begin{smallmatrix} I \\ 0 \end{smallmatrix}\right]$ with the dimensions and partitioning compatible with those of A_2 and A_3, respectively. Pick any F_{s} and L_{s} such that $A_3 + B_{13} F_{\mathrm{s}} E_3'$ and $A_2 + E_2 L_{\mathrm{s}} C_{23}$ are Hurwitz. The following result presents a complete solution of $\mathbf{OP}_1$ in terms of constrained Sylvester equations and AREs, which can be associated with stabilization procedure and L^2 optimization, respectively.

Theorem 1 $\mathbf{OP}_1$ *is solvable iff* A_{1i} *is Hurwitz and there are* Z_2 *and* Z_3 *satisfying*

$$\begin{aligned} A_{3u} Z_2 - Z_2 (A_2 - B_{31} D_2' C_{23}) &= E_3 (A_{13} - B_{11} D_2' C_{23}), \\ (E_3' B_{11} + Z_2 B_{31})\,(I - D_2' D_2) &= 0 \end{aligned}$$

and

$$\begin{aligned} Z_3 A_{2u} - (A_3 - B_{13} D_3' C_{11}) Z_3 &= (A_{13} - B_{13} D_3' C_{13}) E_2, \\ (I - D_3 D_3')\,(C_{13} E_2 + C_{11} Z_3) &= 0, \end{aligned}$$

respectively. The solution of $\mathbf{OP}_1$ *is then given by*

$$K^{opt} = -\mathrm{e}^{-sh} \left[\begin{array}{c|c} A_{FL} & L \\ \hline F & 0 \end{array}\right] - \left[\begin{array}{c|c} A_{FL} & B_3 \\ \hline F & I \end{array}\right] \Pi \left[\begin{array}{c|c} A_{FL} & L \\ \hline C_2 & I \end{array}\right],$$

where (Hurwitz) $A_{FL} := A + B_3 F + L C_2$, $F := -B_3' X - D_3' C_1$, *and* $L := -Y C_2' - B_1 D_2'$, *where* $X \geq 0$ *and* $Y \geq 0$ *are the stabilizing solutions of the AREs*

$$\begin{aligned} &(A + L_G C_2)' X + X (A + L_G C_2) \\ &\qquad - (X B_3 + C_1' D_3)(B_3' X + D_3' C_1) + C_1' C_1 = 0 \end{aligned}$$

and

$$(A+B_3F_G)Y+Y(A+B_3F_G)' \\ -(YC_2'+B_1D_2')(C_2Y+D_2B_1')+B_1B_1'=0,$$

with $F_G:=F_s\left[\begin{array}{ccc} E_3' & 0 & Z_2 \end{array}\right]$, $L_G:=\left[\begin{array}{ccc} Z_3' & 0 & E_2' \end{array}\right]'L_s$, *and*

$$\Pi:=\boldsymbol{\pi}_h\left\{\left[\begin{array}{cc|c} -(A+B_3F)' & (C_1+D_3F)'C_1Y & XL \\ 0 & -(A+LC_2)' & C_2' \\ \hline B_3' & -D_3'C_1Y & 0 \end{array}\right]\right\}.$$

is the FIR system.

The theorem above provides explicit state-space formulae for the solution of $\mathbf{OP}_1$ based on two Sylvester and two algebraic Riccati equations of the same dimension as in the preview-free case. It is worth mentioning that the first term of $K^{\rm opt}$ is based on the optimal solution of the preview-free version of $\mathbf{OP}_1$. In fact, as manifested by the presence of the delay element, this term "ignores" the existence of previewed information. Availability of preview is accounted by the second term, were the only component that depends on the preview length is the FIR block Π. By applying this result to our problem, the optimal feedforward controller can be constructed. Its behavior is illustrates by simulations in the following subsection.

3.3 Simulation results

The results presented below are obtained for a turbine operating at $V_{\rm nom}=15$ m/sec, $p_{\rm nom}=4$ MW and for the following choice of the weight parameters:

$$k_V=1,\ k_n=1\times10^{-3},\ k_u=1.8\times10^{-2},$$
$$k_F=0.5,\ k_T=1,\ k_w=2\times10^{6},\ k_\beta=1\times10^{-3}.$$

The natural questions when using preview are whether it can yield a noticeable performance improvement, and if so, what is its relation to the preview length. To address these questions, a curve of minimal achievable $||H||_2$ as a function of preview length is presented in Figure 5. It shows that the reasonable

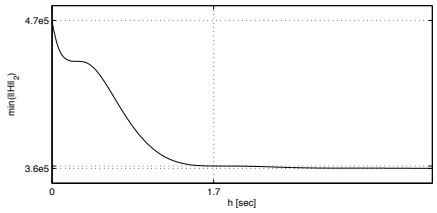

Figure 5: Performance vs. preview length

scale of preview length in our application is a number of seconds. In fact, 98% of possible improvement is achieved with at a preview of 1.7 sec.

Below we will compare the behavior of three systems: 1. without feedforward control; 2. with feedforward control based on local measurements without preview; 3. with feedforward control based on measurements with preview of 1.7 sec. To illustrate the behavior of these systems, we analyze their response to a rectangular pulse in the wind velocity. The pulse starts at the time zero, lasts 1 sec, and has an amplitude of 0.5 m/sec.

Plots of the thrust force, nacelle displacement (tower deflection), pitch angle and rotor speed are presented in Figure 6. We see that feedforward control with

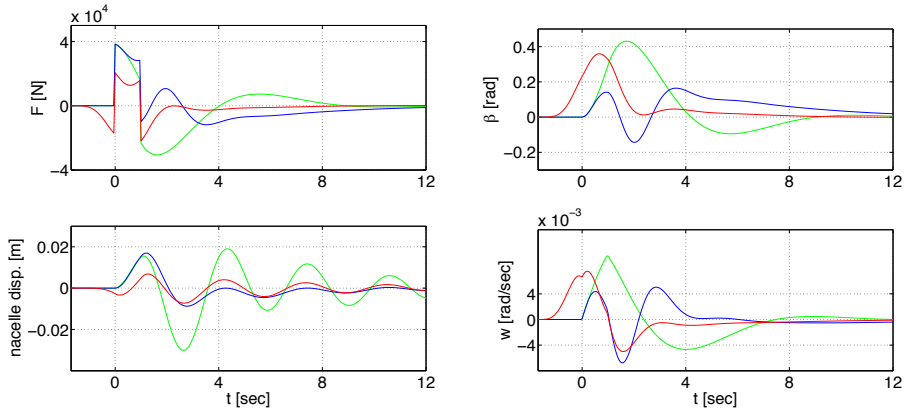

Figure 6: Simulation results: thrust force, nacelle displacement and pitch angle. (green — without feedforward; blue — feedforward without preview; red — feedforward with 1.7 sec preview.)

and without preview substantially damps tower oscillations. Note, however, that once no preview is available, the first peak in the thrust force can not be reduced. This is not a surprise taking into account that the relation between the thrust force and wind speed has a feedthrough term. The resulting immediate force changes can not be compensated by relatively slow pitch dynamics. The benefit of preview is that it offers the controller time to prepare the system prior to the wind gust arrival. Indeed, we see that once preview is available, pitch activity starts before the gust hits the turbine. As a result, the gust arrival is preceded by a drop in the thrust force. This decreases the peak value of the force and also the first peak in tower oscillations. It is worth noting that the reduction in thrust force and tower oscillations is obtained without increasing pitch activity. The feedforward controller changes pitching behavior, yet, the magnitude of pitch angle deviations remains smaller than in the original system. The same observation is true also for rotor speed. The control signal, i.e. power variation, needed to achieve these results is displayed in the left plot in Figure 7.

It is important to mention that in the considered setting the pitch angle can not be changed without affecting the torques. The standard internal con-

troller inevitably transfers power variations to fluctuations in the shaft torque and shaft deflection as displayed in the right plot in Figure 7. Note, however, that the feedforward controller succeeds in alleviating oscillations at the natural frequency of the shaft.

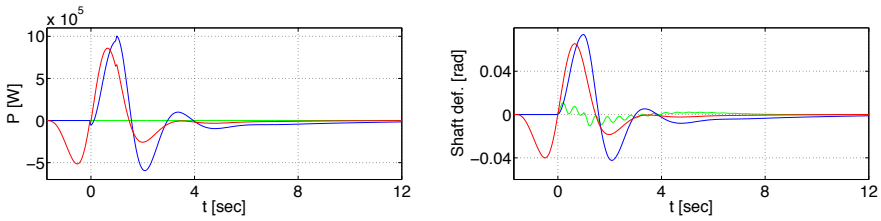

Figure 7: Simulation results: power reference and shaft deflection. (green — without feedforward; blue — feedforward without preview; red — feedforward with 1.7 sec preview.)

Remark 2 *The authors believe that fluctuations of the shaft torque can be reduced once the standard internal controller is omitted. This suggests application of a 2DOF scheme for preview control as in [20], which is a subject of ongoing research.*

In summary of the first part of this report, simulation results demonstrate that, even in presence of standard internal controller, feedforward control based on previewed wind speed measurements can be beneficial. In particular, we saw that short term adjustments in power production can lead to a substantial reduction of tower fluctuations. Moreover, this was achieved without deterioration in terms of pitch activity and rotor speed fluctuations.

4 DISTRIBUTED FEEDFORWARD CONTROL OF THE ENTIRE FARM

Clearly, the control strategy from the previous section can be applied to each of the turbines in the farm. In this setting the i'th turbine controller will generate the control signal u_i based on wind measurements y_i available from the $(i-1)$'th turbine. This situation is depicted in Figure 3 with dashed lines. The downside of this strategy is that adjustments of individual turbine powers result in fluctuations of the overall farm power production. In this section we examine the possibility to alleviate these fluctuations by means of cooperation between the controllers within the control scheme depicted in Figure 3.

4.1 Problem formulation and the associated challenges

In order to address the issues of cooperation between the controllers, we formulate a problem that accounts for overall power production and, as a result,

concerns the entire farm model, described in § 2.2. The signals that should be penalized in the optimization are individual turbine power references $\bar{u}$, outputs $\bar{z}$, defined in (1), and deviation of the overall farm power production, which will be denoted by

$$u_\Sigma := \sum_{i=1}^{N} u_i.$$

Using the notations from § 2.2, the relation between penalized and exogenous signals can be written as

$$\begin{bmatrix} \bar{z}/\bar{w} \\ \bar{u}/\bar{w} \\ u_\Sigma/\bar{w} \end{bmatrix} = \begin{bmatrix} \Lambda G_w \\ 0 \\ 0 \end{bmatrix} + \begin{bmatrix} G_c \\ I \\ \bar{s} \end{bmatrix} \bar{K} D^{-1} \Lambda G_m,$$

where $\bar{s} := \begin{bmatrix} 1 & \dots & 1 \end{bmatrix}$ of an appropriate dimension and

$$\bar{K} := \mathrm{diag}\{K_1, \dots, K_N\}.$$

The cost transfer matrix can now be defined as

$$\bar{H} := \begin{bmatrix} W_{\bar{z}} & 0 & 0 \\ 0 & W_{\bar{u}} & 0 \\ 0 & 0 & W_\Sigma \end{bmatrix} \begin{bmatrix} \bar{z}/\bar{w} \\ \bar{u}/\bar{w} \\ u_\Sigma/\bar{w} \end{bmatrix} W_{\bar{w}},$$

where W_Σ is the weight of the overall power deviation,

$$W_{\bar{z}} := \mathrm{diag}\{W_{z_1}, \dots, W_{z_N}\},\ W_{\bar{u}} := \mathrm{diag}\{W_{u_1}, \dots, W_{u_N}\}$$

contain the weights for all individual turbine outputs and power references, and

$$W_{\bar{w}} := \mathrm{diag}\{W_V, W_{v_1}, \dots, W_{v_N}, W_{n_1}, \dots, W_{n_N}\}$$

contains the weights for all the exogenous input signals. Defining the transfer matrices

$$\left[\begin{array}{c:c} \bar{G}_1 & \bar{G}_3 \\ \hdashline \bar{G}_2 & 0 \end{array}\right] := \left[\begin{array}{c:c} \Lambda W_{\bar{z}} G_w W_{\bar{w}} & W_{\bar{z}} G_c \\ 0 & W_{\bar{u}} \\ 0 & W_\Sigma \bar{s} \\ \hdashline \mathcal{D}^{-1} \Lambda G_m W_{\bar{w}} & 0 \end{array}\right] \tag{4}$$

and choosing the H^2 norm of $\bar{H}$ as the performance criterion, the problem can be formulated as follows.

OP$_2$: Given $\bar{G}_1$, $\bar{G}_2$, $\bar{G}_3$ as defined in (4) find

$$\bar{K} = \mathrm{diag}\{K_1, \dots, K_N\} \in H^\infty,$$

which guarantee

$$\bar{H} = \bar{G}_1 - \bar{G}_3 \bar{K} \bar{G}_2 \in H^2 \cap H^\infty$$

and minimize $||H||_2$.

Similarly to $\mathbf{OP}_1$, the stability requirement $\bar{H} \in H^\infty$ in the formulation above corresponds to asymptotic behavior and minimization of the H^2 norm corresponds to transient performance. However, the conceptual differences of this problem from $\mathbf{OP}_1$ are:

- the constraint on the design parameter $\bar{K}$ to be diagonal;
- the structure of infinite dimensional elements in definitions of G_1 and G_2.

To the best of our knowledge, there are no ready to use solutions of $\mathbf{OP}_2$ in the literature. The challenge of this problem can be associated with the following issues.

1. *Decentralized model matching stabilization.* It is shown in [21] that all stabilizing solutions of a centralized stabilization problem can be characterized by an affine parameterization in terms of a single H^∞ parameter. This result enables one to release stability constraints without changing the structure of the centralized problem. It reduces $\mathbf{OP}_1$ to an L^2 optimization and serves as a preliminary step in the solution of $\mathbf{OP}_1$ in [12]. The question is whether the result of [21] can be extended to the decentralized setting of $\mathbf{OP}_2$. Decentralized model matching stabilization was considered in [22] in the context of a decoupling problem. Yet, the solution proposed there is not readily applicable to $\mathbf{OP}_2$, since it does not reveal the structure of parameterization of stabilizing solutions.

2. *Decentralized model matching optimization.* This problem is of a general interest in the context of distributed control and the notion of quadratic invariance, [23]. Any quadratically invariant problem can be reduced to model matching setup with a structural constraint on the Youla parameter. This constraint can always be transformed into diagonality constraint, following the idea from [24]. Explicit state-space formulae for one special case of a structural constraint were derived in [25]. The question is whether a similar analytical solution can be found for the general decentralized setting of $\mathbf{OP}_2$. A preliminary frequency domain solution is presented in the following subsection. Yet, this result is in a sense implicit, as it does not reveal the order and the structure of the optimal solution. So the problem remains open.

3. *Structure of infinite dimensional elements.* Typically, wind propagation delays between adjacent turbine are much larger compared to the time constants of turbine dynamics. As a result, discretizing the time axes and absorbing delays into the dynamics of G_2 and G_1 will substantially increase the order of these systems. In the case of a large-scale farm, this will result in numerically unfeasible solutions. The question is whether there exists a solution to $\mathbf{OP}_2$ with similar properties as the solution of $\mathbf{OP}_1$. Namely, a solution whose computational burden does not depend on the length of the delays.

The issues listed above are subject to ongoing research. Meanwhile, in order to assess the potential of the proposed distributed feedforward control scheme, an approximate solution of $\mathbf{OP}_2$ will be presented in the following subsection.

4.2 Decentralized model matching and Hadamard product

Unstable poles in $\mathbf{OP}_2$ stand for dynamics of external signals and modes and are located on the imaginary axes. Thus, the stabilization part of the problem can be circumvented by shifting the unstable poles by a small deviation ϵ into the open left half plane. This will have small influence on the optimal solution, but will eliminate the stability constraint by guaranteeing $\bar{H} \in H^\infty$. Motivated by this we will assume hereafter that

$\boldsymbol{\mathcal{A}_4}$: $\bar{G}_1$, $\bar{G}_2$ and $\bar{G}_3$ are stable.

We will assume also that

$\boldsymbol{\mathcal{A}_5}$: $\bar{G}_1(\infty) = 0$,

$\boldsymbol{\mathcal{A}_6}$: $\bar{G}_{2/3}(\infty)$ have full row/column rank respectively,

$\boldsymbol{\mathcal{A}_7}$: $\bar{G}_{2,3}$ have no purely imaginary transmission zeros.

Assumption $\boldsymbol{\mathcal{A}_5}$ is technical and imposes no loss of the generality. Indeed, $\mathbf{OP}_2$ is solvable only if there exists $\bar{K}$ that renders $\bar{H} \in H^2$ and, in particular, guarantees that $\bar{H}(\infty) = 0$. This, in turn, is possible only if there exists a diagonal matrix D_k such that $\bar{G}_1(\infty) - \bar{G}_3(\infty)D_k\bar{G}_2(\infty) = 0$. In this case, the design parameter can be shifted as $\tilde{K} := \bar{K} - D_k$ to yield a problem in which $\boldsymbol{\mathcal{A}_5}$ is satisfied. The assumptions $\boldsymbol{\mathcal{A}_6}$ and $\boldsymbol{\mathcal{A}_7}$ are standard and rule out problem redundancy and singularity. Following the same arguments as in [12, § II], the domain of the optimization parameter $\bar{K}$ can now be replaced by

$$H_D^2 := \{\mathrm{diag}\{K_1, \ldots, K_N\} \mid K_1, \ldots, K_N \in H^2\}.$$

At this point, the problem can be effectively rewritten as

$$\bar{K}^* = \underset{\bar{K} \in H_D^2}{\mathrm{argmin}} ||\bar{G}_1 - \bar{G}_3\bar{K}\bar{G}_2||_2. \tag{5}$$

Below we will derive a solution of (5) using Khatri-Rao product and its properties, as proposed in [14]. Applying vec operator to (5), we can reshape it as

$$\mathrm{vec}(\bar{K}^*) = \underset{\bar{K} \in H_D^2}{\mathrm{argmin}} ||\mathrm{vec}(\bar{G}_1) - \mathrm{vec}(\bar{G}_3\bar{K}\bar{G}_2)||_2.$$

Using properties of Kronecker product, [26], the last expression can be rewritten as

$$\mathrm{vec}(\bar{K}^*) = \underset{\bar{K} \in H_D^2}{\mathrm{argmin}} ||\mathrm{vec}(\bar{G}_1) - (\bar{G}_2' \otimes \bar{G}_3)\mathrm{vec}(\bar{K})||_2. \tag{6}$$

Note that since $\bar{K}$ is constrained to be diagonal, the column $\mathrm{vec}(\bar{K})$ is sparse. The zero elements of $\mathrm{vec}(\bar{K})$ point out on the redundant columns of $\bar{G}_2' \otimes \bar{G}_3$,

which do not influence $\bar{H}$. Erasing these irrelevant columns, the Kronecker product in (6) turns into Khatri-Rao product and we get

$$\mathrm{dvec}(\bar{K}^*) = \underset{\bar{K}\in H_D^2}{\mathrm{argmin}} ||\mathrm{vec}(\bar{G}_1) - (\bar{G}_2' \odot \bar{G}_3)\mathrm{dvec}(\bar{K})||_2.$$

Denoting

$$\tilde{K} := \mathrm{dvec}(\bar{K}),\ \tilde{G}_1 := \mathrm{vec}(\bar{G}_1),\ \tilde{G}_3 := (\bar{G}_2' \odot \bar{G}_3)$$

the problem can be rewritten as

$$\tilde{K}^* = \underset{\tilde{K}\in H^2}{\mathrm{argmin}} ||\tilde{G}_1 - \tilde{G}_3\tilde{K}||_2. \tag{7}$$

This way, using the notion of Khatri-Rao product, the original problem is reduced to a standard one-side model matching optimization with no structural constraint on the parameter (7). Let us introduce spectral factorization

$$U_3^{\sim} U_3 = \tilde{G}_3^{\sim}\tilde{G}_3, \quad U_3, U_3^{-1} \in H^\infty.$$

Note that due to the properties of Khatri-Rao product, [26],

$$\tilde{G}_3^{\sim}\tilde{G}_3 = (\bar{G}_2' \odot \bar{G}_3)^{\sim}(\bar{G}_2' \odot \bar{G}_3) = (G_2 G_2^{\sim})' \circ (G_3^{\sim} G_3).$$

At this point, standard Hilbert space arguments can be applied as in [12] to derive the solution of (7)

$$\tilde{K}^* = U_3^{-1}\{U_3^{-\sim}\tilde{G}_3^{\sim}\tilde{G}_1\}_-$$

and the corresponding minimal achievable norm

$$||\tilde{G}_1 - \tilde{G}_3\tilde{K}^*||_2 = ||\{U_3^{-\sim}\tilde{G}_3^{\sim}\tilde{G}_1\}_+||_2.$$

The following result can now be formulated.

Theorem 2 *Let the assumptions* $\boldsymbol{\mathcal{A}_{5\text{-}7}}$ *hold. Then,* $\mathbf{OP}_2$ *is solvable and the optimal* $\bar{K}$ *with the corresponding minimal* $||\bar{H}||_2$ *are given by*

$$dvec(\bar{K}^*) = U_3^{-1}\{U_3^{-\sim}(\bar{G}_2' \odot \bar{G}_3)^{\sim} vec(\bar{G}_1)\}_-,$$
$$min||\bar{H}^*||_2 = ||\{U_3^{-\sim}(\bar{G}_2' \odot \bar{G}_3)^{\sim} vec(\bar{G}_1)\}_+||_2,$$

where U_3 *is a spectral factor satisfying*

$$U_3^{\sim} U_3 = (G_2 G_2^{\sim})' \circ (G_3^{\sim} G_3), \quad U_3, U_3^{-1} \in H^\infty.$$

The theorem above constitutes a frequency domain solution of $\mathbf{OP}_2$ under assumptions $\boldsymbol{\mathcal{A}_{5\text{-}7}}$. The solution is given in terms of spectral factorization of Hadamard product of transfer matrices associated with the centralized problem. Note that despite the use of Kronecker product in derivations, the dimension of the resulting spectral factorization is compatible with the dimensions of the original problem data. The order of the factorization, however, is infinite due to delays involved in the problem. Thus, in order to get the preliminary simulation results, presented in the following subsection, the time axis has to be discretized.

Remark 3 *Even for finite order problems (without delays), the result of Theorem 2 does not reveal the order of the optimal solution and its structure. Yet, it can be considered as a first step towards derivation of explicit analytic solution of* $\mathbf{OP}_2$. *The main deficiency at this point is in convenient state-space formulae for the Hadamard product.*

4.3 Preliminary simulation results

To illustrate application of the proposed control scheme, we consider a farm consisting of $N = 5$ turbines with an incoming mean wind speed of $V_{\text{nom}} = 15$ m/s. We choose the power set point for the farm as $P_{\text{farm}} = 17$ MW and distribute the powers among the turbines as in [7]:

$$P_{\text{nom}_1} = P_{\text{nom}_2} = 4 \text{ MW}, \; P_{\text{nom}_3} = P_{\text{nom}_4} = P_{\text{nom}_5} = 3 \text{ MW}.$$

The nominal wind speeds experienced by each of the turbines are computed according to the static model in [17]

$$V_{\text{nom}_1} = 15 \; \frac{\text{m}}{\text{sec}}, \quad V_{\text{nom}_2} = 14.7 \; \frac{\text{m}}{\text{sec}}, \quad V_{\text{nom}_3} = 14.5 \; \frac{\text{m}}{\text{sec}},$$
$$V_{\text{nom}_4} = 14.42 \; \frac{\text{m}}{\text{sec}}, \quad V_{\text{nom}_5} = 14.37 \; \frac{\text{m}}{\text{sec}}.$$

We choose the weights for input and output signals of each turbine to be the same as in Section 3, up to the shift of imaginary axis poles by $\epsilon = 0.01$. The weight for the overall farm power production is chosen to be static $W_\Sigma = 0.1$. We assume that the wind propagation delay is $h = 2$ sec. Note that this value is not typical for real wind farms, where the delays are considerably longer. We choose h to be small in order to avoid numerical problems related to discretization of the time axis, which is necessary for application of the approximate solution from the previous subsection. Hence, the results presented below serve illustration purposes only. Our aim here is to explain what kind of cooperation can be achieved under the proposed control scheme and what the benefits of such a cooperation are.

To facilitate further explanations denote the controllers obtained by solving $\mathbf{OP}_2$ by $\mathcal{K}_i$ for $i = 1 \dots 5$. Denote the "non-cooperative" controllers obtained by solving $\mathbf{OP}_1$ for each individual turbine by $\tilde{\mathcal{K}}_i$ for $i = 1 \dots 5$.

To get the first insight into the behavior of distributed feedforward control scheme, let us consider impulse responses of the optimal controllers. Impulse responses of $\mathcal{K}_1$ and $\mathcal{K}_5$ are presented in Figure 8, where they are compared to those of $\tilde{\mathcal{K}}_1$ and $\tilde{\mathcal{K}}_5$. Note that the impulse response of $\mathcal{K}_1$ differs from that of $\tilde{\mathcal{K}}_1$ by sharp peaks occurring at the time multiples of h. These peaks reflect the fact that $\mathcal{K}_1$ "expects" downwind turbines to experience similar wind fluctuations as the first turbine, but with delays of h sec, $2h$ sec and so on. To take this into account, $\mathcal{K}_1$ adjusts the power production of the first turbine at the right times in order to compensate for anticipated power changes of its downwind neighbors. The same behavior is also present in impulse responses of $\mathcal{K}_2, \dots, \mathcal{K}_4$, which have been omitted due to space limitations. The number of

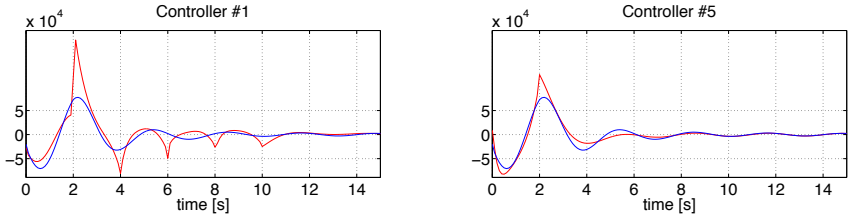

Figure 8: Impulse responses of $\mathcal{K}_1$, $\tilde{\mathcal{K}}_1$ (left) and $\mathcal{K}_5$, $\tilde{\mathcal{K}}_5$ (right). (blue — $\tilde{\mathcal{K}}_1$, $\tilde{\mathcal{K}}_5$; red — $\mathcal{K}_1$, $\mathcal{K}_5$)

peaks in their impulse responses relates to the number of downwind turbines. Since the fifth turbine is the last one in the row, the only peak in the impulse response of $\mathcal{K}_5$ corresponds to its own preview window.

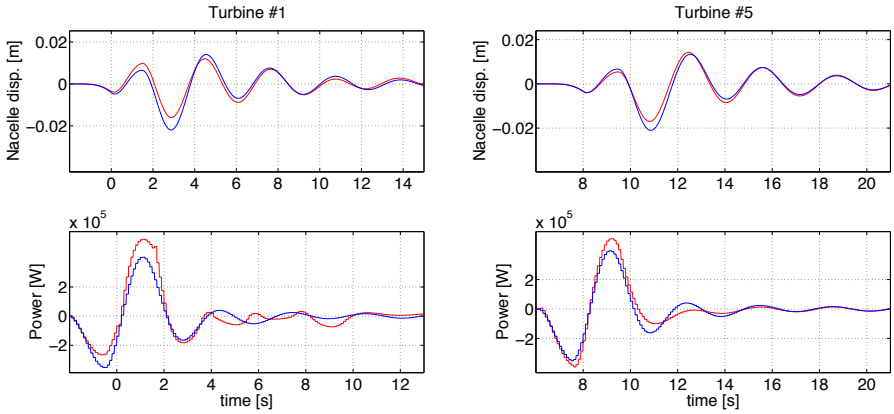

Figure 9: Simulation results: Nacelle displacements and power deviations of the first turbine (left) and the last turbine (right). (blue — feedforward with $\tilde{\mathcal{K}}_i$; red — feedforward with $\mathcal{K}_i$)

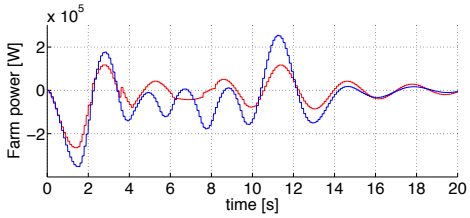

Figure 10: Simulation results: Variation in overall wind farm power (blue — feedforward with $\tilde{\mathcal{K}}_i$; red — feedforward with $\mathcal{K}_i$)

As in Section 3.3, we study the system's response to an incoming wind gust.

We assume that the wind gust starts at time zero, lasts 1.5 sec and has an amplitude of 0.5 m/s. Figure 9 shows nacelle displacement and power production of the first and the last turbine. We see that cooperation between controllers accommodates more aggressive control actions. As a result cooperative controllers slightly reduce tower oscillations compared to noncooperative ones. This comes at the expense of individual turbine power variations. However, the main benefit of considering the whole farm ($\mathcal{K}_i$ via $\mathbf{OP}_2$) rather then individual turbines ($\tilde{\mathcal{K}}_i$ via $\mathbf{OP}_1$) becomes evident once the overall farm power production is examined, see Figure 10. We observe that cooperation between turbines significantly reduces fluctuations in the overall farm power production without causing deterioration in terms of load reduction.

5 SUMMARY

In this report a problem in wind farm control for load mitigation was addressed. A distributed feedforward control scheme was considered, in which the wind speed measurements from upwind turbines are transmitted to their closest downwind neighbors. Potential benefits of this control scheme were illustrated using a simple setup of one row of collective pitch turbines with standard internal controllers.

In the first part of the report the problem of using previewed wind speed measurements was considered. It was formulated as H^2 model matching optimization and solved using the result from [12]. Simulation results were presented indicating reduction of thrust force and tower oscillations and motivating application of preview control techniques to a more general setting without an internal controller. In the second part of the report the possibility of cooperation between turbines was considered. The problem was formulated as H^2 decentralized model matching optimization and a number of open theoretical challenges associated with it were discussed. An approximate frequency domain solution of the problem was presented and the benefits of cooperation were illustrated by simulations.

References

[1] "Wind is a global power source," Global Wind Energy Council, http://www.gwec.net/index.php?id=13, Accessed 27/09/2011.

[2] L. Y. Pao and K. E. Johnson., "A tutorial on the dynamics and control of wind turbines and wind farms," in *Proceedings of American Control Conference*, June 2009, pp. 2076–2089.

[3] T. Burton, D. Sharpe, N. Jenkins, and E. Bossayani, *Wind Energy Handbook*. John Wiley & Sons, 2008.

[4] S. Frandsen, "Turbulence and turbulence generated structurual loading in wind turbine clusters," Ph.D. dissertation, Riso National Laboratory, Denmark, 2007.

[5] E. A. Bossanyi, "Wind turbine control for load reduction," *Wind Energy*, vol. 6, pp. 229–244, 2003.

[6] K. Hammerum, P. Brath, and N. K. Poulsen, "A fatigue approach to wind turbine control," *Journal of Physics: Conference Series*, vol. 75, 2007.

[7] D. Madjidian, K. Martensson, and A. Rantzer, "A distributed coordination scheme for fatigue load minimization in wind farm," in *Proceedings of American Control Conference*, June 2011.

[8] R. Frehlich and N. Kelley, "Measurements of wind and turbulence profiles with scanning doppler lidar for wind energy applications," *IEEE Journal of Selected Topics in Applied Earth Observations and Remote Sensing*, vol. 1, no. 1, pp. 42–47, March 2008.

[9] J. H. Laks, L. Y. Pao, and A. D. Wright, "Control of wind turbines: Past, present, and future," in *Proceedings of American Control Conference'*, July 2009, pp. 2096–2103.

[10] J. Laks, L. Pao, A. Wright, N. Kelley, and B. Jonkman, "The use of preview wind measurements for blade pitch control," *Mechatronics*, in press, 2011.

[11] D. Schlipf, S. Schuler, F. Allgower, and M. Kuhn, "Look-ahead cylcic pitch control with lidar," in *Proc. of Torque*, June 2010.

[12] M. Kristalny and L. Mirkin, "On the H^2 two-side model matching with preview," in *Proc. 19th MTNS Symposium*, Budapest, Hungary, 2010.

[13] V. Spudic, M. Jelavic, M. Baotic, and N. Peric, "Hierarchical wind farm control for power/load optimization," in *Proc. of Torque*, Heraklion, Greece, June 2010.

[14] K. Park, "H^2 design of one-degree-of-freedom decoupling controllers for square plants," *International Journal of Control*, vol. 81, no. 2, pp. 1343–1351, Sep. 2008.

[15] J. Jonkman, S. Butterfield, W. Musial, and G. Scott, "Definition of a 5-mw reference wind turbine for offshore system development." National Renewable Energy Laboratory, Golden, Colorado, Tech. Rep., Feb 2010.

[16] T. Knudsen, "Validated dynamic flow model," Aeolus Deliverable 2.5, Tech. Rep., 2011.

[17] D. Madjidian and A. Rantzer, "A stationary model for control of wind farms," in *Proceedings of the 18th IFAC World Congress*, 2011.

[18] M. Tomizuka, "Optimal continuous finite preview problem," *IEEE Transactions On Automatic Control*, vol. 20, no. 3, pp. 362–365, 1975.

[19] A. A. Moelja and G. Meinsma, "H^2 control of preview systems," *Automatica*, vol. 42, no. 6, pp. 945 – 952, 2006.

[20] M. Kristalny and L. Mirkin, "Preview in H^2 optimal control: Experimental case studies," in *49th IEEE Conference on Decision and Control*, Atlanta, GA, Dec. 2010.

[21] ——, "On the parameterization of stabilizing solutions to general four-block model matching problems," in *submitted to SIAM Journal on Control and Optimization*, 2011.

[22] K. Park, "Existence conditions of decoupling controllers in the generalized plant model," in *47th IEEE Conference on Decision and Control*, Cancun, Mexico, Dec. 2008, pp. 5158–5163.

[23] M. Rotkowitz and S. Lall, "A characterization of convex problems in decentralized control," *IEEE Transactions On Automatic Control*, vol. 51, no. 2, pp. 1984–1996, Feb 2006.

[24] M. Rotkowitz, "Parametrization of all stabilizing controllers subject to any structural constraint," in *49th IEEE Conference on Decision and Control*, Dec. 2010, pp. 108–113.

[25] J. Swigart and S. Lall, "Optimal synthesis and explicit state-space solution for a decentralized two-player linear-quadratic regulator," in *49th IEEE Conference on Decision and Control*, Atlanta, GA, Dec. 2010.

[26] J. W. Brewer, "Kronecker products and matrix calculus in systems theory," *IEEE Transactions On Circuits And Systems*, vol. cas-25, no. 9, pp. 772–781, 1978.